JACS Au
AN OPEN ACCESS JOURNAL OF THE AMERICAN CHEMICAL SOCIETY

pubs.acs.org/jacsau

Letter

Redox-Switchable Allosteric Effects in Molecular Clusters

Benjamin S. Mitchell, Sebastian M. Krajewski, Jonathan A. Kephart, Dylan Rogers, Werner Kaminsky, and Alexandra Velian*

Cite This: *JACS Au* 2022, 2, 92–96

Read Online

ACCESS | Metrics & More | Article Recommendations | Supporting Information

ABSTRACT: We demonstrate that allosteric effects and redox state changes can be harnessed to create a switch that selectively and reversibly regulates the coordination chemistry of a single site on the surface of a molecular cluster. This redox-switchable allostery is employed as a guiding force to assemble the molecular clusters $Zn_3Co_6Se_8L'_6$ (L′ = $Ph_2PN(H)Tol$, Ph = phenyl, Tol = 4-tolyl) into materials of predetermined dimensionality (1- or 2-D) and to encode them with emissive properties. This work paves the path to program the assembly and function of inorganic clusters into stimuli-responsive, atomically precise materials.

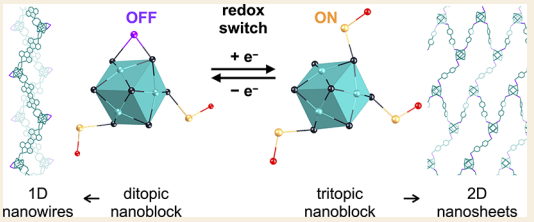

KEYWORDS: *allosteric site-differentiation, redox switch, atomically precise, inorganic clusters, cluster assembled nanomaterials*

Reversibly activating a single coordination site on the surface of an inorganic cluster could enable unprecedented control over reactivity, opening uncharted paths for catalyst development and functional materials synthesis.[1,2] While redox cooperativity and charge redistribution among neighboring metals have been shown to lead to site-selective reactivity in some molecular clusters,[3−5] reversibly regulating the coordination chemistry of a single site on the surface of a molecular cluster remains elusive. More often, chemical differentiation, achieved either using the supporting ligand or by changing the identity of the metal itself, is required to direct the chemistry to a single site.[6−15] On an extended surface, the reactivity of chemically degenerate surface sites can become differentiated as a result of ligand binding via "inter-adsorbate interactions", giving rise to important phenomena such as altered Sabatier volcano curves[16,17] or nanopatterning.[18] When a substrate binds at one site on a surface, it induces subtle structural and electronic changes at neighboring sites that alter their reactivity primarily by modifying adsorption energies. For example, inter-adsorbate interactions inhibit CO adsorption at nearest-neighbor sites on Cu(100) due to decreased electron density around the initial CO adsorption site.[19] Similar effects are invoked as the major contributors for the coverage-dependent adsorption energy of H_2S on FeS_2.[20] Inspired by inter-adsorbate effects in extended materials, we set out to probe if site-differentiation of a molecular cluster could also be achieved based solely on ligand binding and to investigate if redox state changes can be used as a switch for this differentiation.

Our group previously introduced a family of molecular clusters $M_3Co_6Se_8L'_6$ (**M$_3$**, L′ = $Ph_2PN(H)R$, Ph = phenyl, R = 4-tolyl; **M$_3$***, R = isopropyl, M = Fe, Co, Zn, Sn) with three degenerate surface sites (M) that can engage with substrates and linkers,[21−24] enabling them to function as catalysts[21] and building blocks alike.[23] In this study, a redox innocent metal, Zn, was selected to decorate the cluster; therefore, a redox change in the Co_6Se_8 support would be unambiguously responsible for modifying the affinity of the cluster for linkers. Two main discoveries were made. First, the equivalent edge sites of **Zn$_3$** become site-differentiated when exposed to ligands (Scheme 1). This is an illustration of inter-adsorbate effects

Scheme 1. Redox-Switchable Allosteric Effects: A Powerful Strategy to Reversibly Site-Differentiate Degenerate Surface Sites in Inorganic Clusters

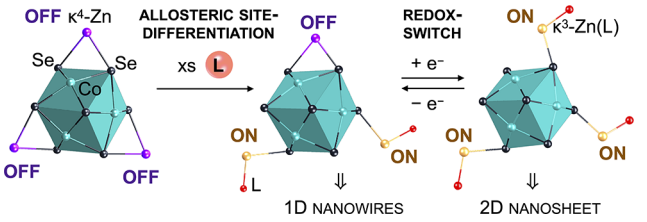

wherein through-cluster electronic and structural rearrangements are propagated between the edge Zn sites upon ligand binding. Due to its similarity to allosteric effects in biological systems,[25,26] we refer to it as allosteric site-differentiation. Second, the site-differentiation can be reversibly switched "on" or "off" by simply changing the oxidation state of the cobalt

Received: November 4, 2021
Published: December 20, 2021

https://doi.org/10.1021/jacsau.1c00491
JACS Au 2022, 2, 92–96

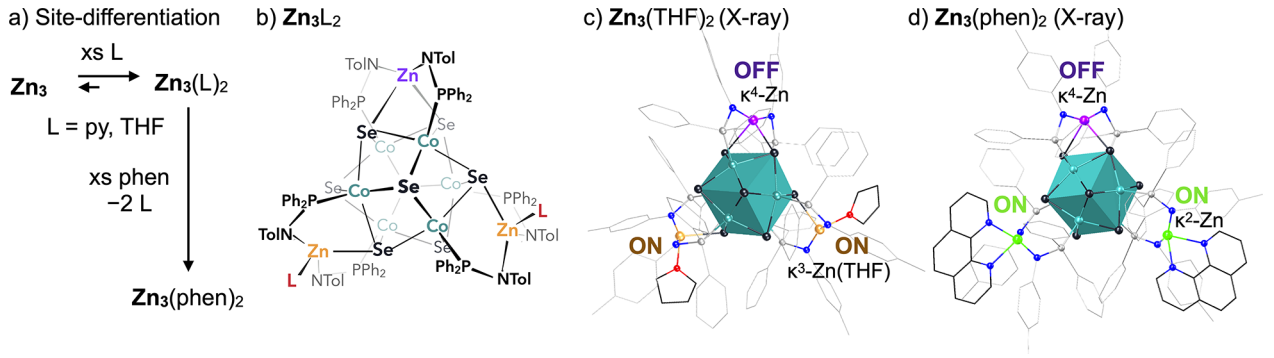

Figure 1. (a) Synthesis of a ditopic nanoblock and (b) structure of Zn_3L_2 (L = THF or py). Single crystal X-ray diffraction structures of (c) $Zn_3(THF)_2$ and (d) $Zn_3(phen)_2$. Hydrogen atoms, cocrystallized solvent, and any disorder are omitted for clarity.

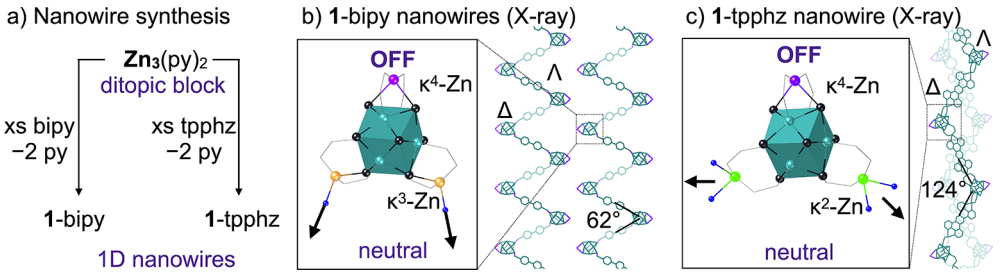

Figure 2. (a) Synthesis of nanowires **1**-bipy and **1**-tpphz. Single crystal X-ray data of (b) **1**-bipy and (c) **1**-tpphz, with insets depicting a single cluster node of Δ-helicity. Organic ligands, hydrogen atoms, and any cocrystallized solvent are not depicted for clarity.

selenide support. The utility of this redox-switchable allosteric effect is illustrated in the assembly of the atomically precise materials of predetermined dimensionality, namely one-dimensional nanowires and two-dimensional nanosheets. While electrons are a convenient way to operate a molecular switch, we also demonstrate that an inner-sphere electron transfer pathway relying on quinone reduction can be employed to tag the Zn_3 nanocluster. We use this strategy to equip the ditopic nanocluster building block Zn_3L_2 with a fluorophore, opening a new path to access stimuli-responsive, atomically precise nanomaterials.[27−29]

Zn_3 is prepared by salt metathesis from $Li_6(py)_6Co_6Se_8L'_6$ (1.0 equiv) and $ZnCl_2$ (3.3 equiv).[21,22] In the presence of coordinating ligands (L), the cluster is isolated exclusively as the site-differentiated bis-adduct Zn_3L_2 (L = py; 4.5 g, 80% yield, Figure 1a and b). Single crystal X-ray diffraction shines light on the site-differentiation, revealing an allosteric effect in which THF binding at two of the Zn edge sites effectively strengthens the Zn−Co_6Se_8 interactions at the third. Two Zn(THF) sites are chelated κ^3 by the cluster via two amides and one Se, while the third is bound κ^4, featuring a second Zn−Se bond (Figure 1c). The site-differentiation is retained in the presence of excess 1,10-phenanthroline (phen), a chelating ligand with strong σ-donating properties. In the solid state, the bis-adduct $Zn_3(phen)_2$ (78% yield; Figure 1a) features one naked κ^4-Zn edge and two κ^2-Zn sites in which both Zn−Se interactions have been replaced by coordination to phenanthroline (Figure 1d).[30−32] The allosteric effect set off by ligand binding in Zn_3 is enabled by the hemilability of the metal−support interactions.[21,22] We propose that breaking a Zn−Se bond upon ligand coordination begins a cascading effect through the Co_6Se_8 support which regains some electron density and presents at another Zn edge site by strengthening the Zn−Se interaction and diminishing its affinity for exogenous ligands.

Here, the utility of the site-differentiation is harnessed to control the dimensionality of cluster-assembled nanostructures. Typically, the chemically degenerate sites on the surface of inorganic clusters bind linkers indiscriminately, precluding dimensional control over the assembly. Synthetic pathways that enable deterministic assembly routes of low-dimensional structures are an active area of research.[23,33−36] With only two edge sites available to engage linkers, the $Zn_3(py)_2$ cluster is poised to encode the formation of a one-dimensional wire when mixed with a linear ditopic ligand. To mimic the coordination of pyridine and phenanthroline at the Zn edge sites, two types of nitrogen based linear linkers are employed: the monodentate 4,4′-bipyridine (bipy) and the chelating tetrapyrido[3,2-a:2′,3′-c:3″,2″-h:2‴,3‴-j] phenazine (tpphz), respectively. Black, prismatic crystals of the nanowires $[Zn_3(bipy)]_n$ (**1**-bipy, 48% yield) and $[Zn_3(tpphz)]_n$ (**1**-tpphz, 65% yield) grew over the course of 2−3 days of mixing $Zn_3(py)_2$ with excess bipy or tpphz (Figure 2a). Single crystal X-ray diffraction reveals the similarity of the cluster nodes with their molecular counterparts, which retain one edge site in the "off", κ^4-Zn state, and two linker-bound edge sites that enable catenation of the wires (Figure 2b and c). While both nanowires exhibit a zigzag motif, the κ^2-Zn versus κ^3-Zn linkages produce obvious structural differences. Most notably, the kinks of the wire measure 62° in **1**-bipy and double, 124°, in **1**-tpphz, where the chelating effect of tpphz disengages the Zn from the cluster enabling a more relaxed chain. Interestingly, in both wires, the racemic mixture of helical nanoclusters (Λ, Δ) of Zn_3 assembles with alternating enantiomers, giving rise to the first examples of syndiotactic nanocluster wires. Typically, the tacticity of hybrid inorganic/organic polymers is encoded based on the chirality of the organic linker rather than the intrinsic chirality of an inorganic node.[37−39] Tacticity in organic polymers is associated with drastic differences in physical properties; exploring the

https://doi.org/10.1021/jacsau.1c00491
JACS Au 2022, 2, 92−96

consequences of tacticity in inorganic hybrid materials could likewise be tied to interesting properties, but in part due to lack of synthetic access, this remains a little explored frontier.

We previously observed that oxidation state changes affect the affinity for ligands of Fe_3 clusters.[21] Here, we set out to explore if an increased affinity for ligands upon oxidation could turn the κ^4-Zn site into a redox switch. Electrochemically, Zn_3 exhibits three single electron oxidation events (−0.37, 0.12, and 0.49 V) and one reduction (−1.59 V) all of which are chemically reversible (Figures S16–S18; referenced to Fc/Fc^+). The chemical oxidation of the neutral bis-adduct $Zn_3(py)_2$ in the presence of phenanthroline (3.3 equiv) is revealing. The tris-adduct $[Zn_3(phen)_3][PF_6]$ (80%; Figure 3a) is formed as the sole product, and its solid state structure

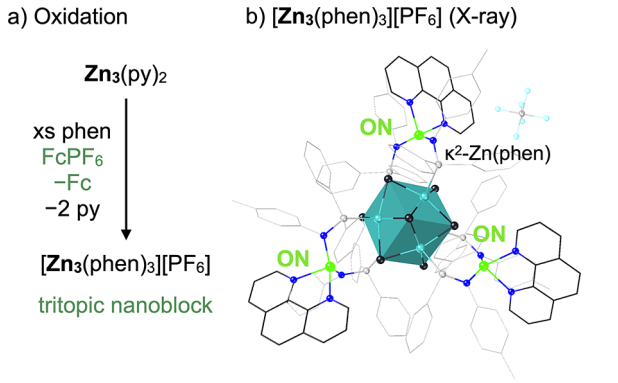

Figure 3. (a) Synthesis of a tritopic nanoblock. (b) Single crystal X-ray diffraction structure of $[Zn_3(phen)_3][PF_6]$. Hydrogen atoms, cocrystallized solvent, and any disorder are omitted for clarity.

confirms the chemical equivalence of its three κ^2-Zn edge sites (Figure 3b). The formation of $[Zn_3(phen)_3]^+$ illustrates how removing a single electron from the cobalt core can be used to switch "on" the affinity for ligands at the κ^4-Zn site in the neutral cluster $Zn_3(phen)_2$. Due to the redox resilience of the Co_6Se_8 support, this process is electrochemically reversible (Figure S17). The ability to switch between the neutral and mono-oxidized nanoclusters using electrons in the transformation $Zn_3(L)_2 + L \rightleftharpoons [Zn_3(L)_3]^+ + e^-$ makes the zinc nanocluster an exceptional candidate for the assembly of stimuli-responsive materials.

Redox-switching "on" the affinity for ligands at the κ^4-Zn site turns the ditopic $Zn_3(py)_2$ cluster into a tritopic nanoblock, which in combination with linear linkers would give rise to two-dimensional nanosheets. Mixing the $Zn_3(py)_2$ nanocluster, the $FcPF_6$ oxidant, and the bipy linker gives rise over the course of 2 days to black, prismatic crystals identified as $[Zn_3(bipy)_{1.5}][PF_6]$ (**2**-bipy, 44% yield; Figure 4a). This material is identified as a layered two-dimensional van der Waals material, with each nanoblock in the +1 oxidation state, using single crystal X-ray diffraction (Figure 4b). The structure of the individual nanosheets is remarkably similar to that of the previously reported $Co_3(bipy)_{1.5}Co_6Se_8L'_6$ nanosheet,[23] with the only major differences being the presence of the PF_6^- anion and the orientation of the sheets within the crystal lattice.

Beyond controlling dimensionality, electron transfer can be used to endow $Zn_3(py)_2$ with orthogonal emissive properties. The ruthenium complex $[Ru(bipy')_2(phendione)][PF_6]_2$ (bipy′ = 2,2′-bipyridine, phendione = 1,10-phenanthroline-

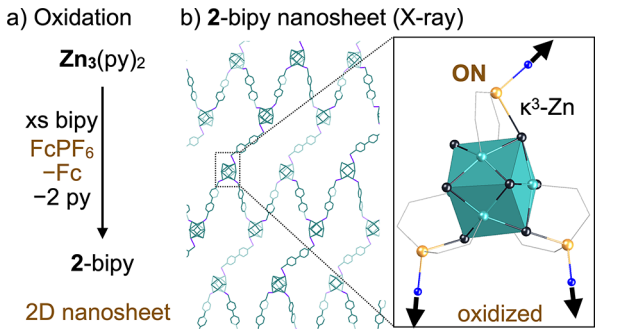

Figure 4. (a) Synthesis of **2**-bipy nanosheets. (b) Single crystal X-ray diffraction structure of **2**-bipy, with an inset depicting a tritopic node of Δ-helicity. Counterion PF_6^-, organic ligands, hydrogen atoms, and any cocrystallized solvent are not depicted for clarity.

5,6-dione) is uniquely equipped to serve as both a fluorophore and an inner-sphere oxidant due to the dione moiety.[40−42] Treatment of $Zn_3(py)_2$ (1 equiv) with $[Ru(bipy')_2(phendione)][PF_6]_2$ (1 equiv) produces a new species **3** (Figure 5), which is most consistent with the structure

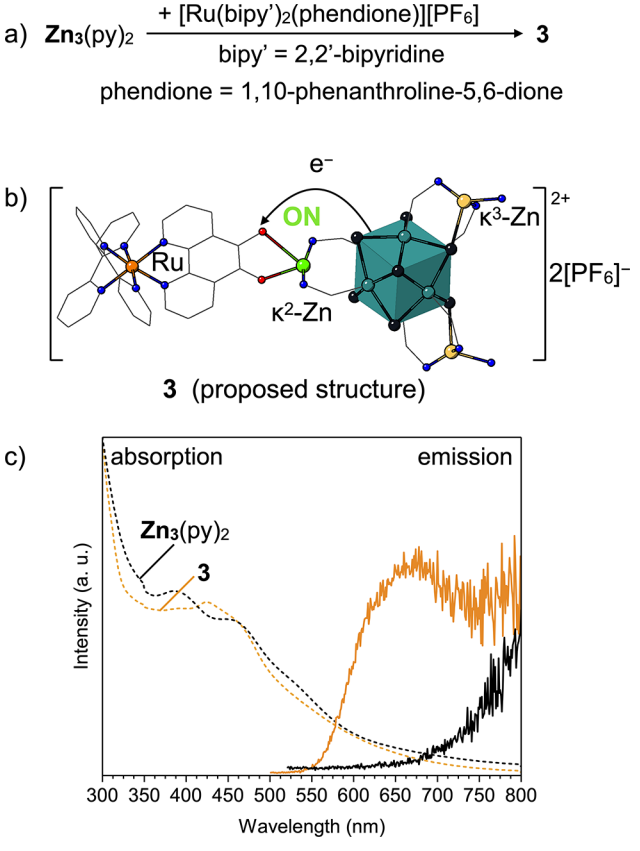

Figure 5. (a) Synthesis of **3** and (b) structural model highlighting the inner-sphere electron transfer from the cobalt core to the phendione unit. (c) Absorption and emission (438 nm excitation) profiles of **3** and $Zn_3(py)_2$.

proposed in Figure 5b. Signaling the oxidation of the Co_6Se_8 core is the emergence of a single paramagnetic ^{31}P NMR resonance in **3** at −415 ppm. The monoreduction of the quinone to a semiquinone is reflected in the disappearance of the C═O stretch (1770 cm^{-1}) of the starting material and the appearance of a lower energy feature at 1464 cm^{-1}, attributed

https://doi.org/10.1021/jacsau.1c00491
JACS Au 2022, 2, 92−96

to the C−O stretch.[41,43] Upon excitation at λ_{max} (438 nm), **3** exhibits a broad emission band centered at 677 nm. Not only is this feature absent in $\mathbf{Zn_3}(py)_2$, but it is 50 nm red-shifted from the parent Ru complex (Figure 5c). Preliminary studies reveal that **3** has potential as a nanoblock; treating it with bipy results in the formation of a material insoluble in common organic solvents—the hallmark of an extended framework.

Traditionally, allosteric effects describe how the binding of a ligand at one site of a protein alters the properties of a distant site on the same protein.[25,26] In $\mathbf{Zn_3}$, ligand binding at one edge site sets off a domino effect that changes the affinity for ligands at another Zn site. The hemilability of the interactions between the edge (Zn) and the redox-active support (Co_6Se_8) enables the creation of a switch, wherein electron transfer controls the affinity for ligands at a single Zn edge site. The redox-switchable allosteric site-differentiation of the $\mathbf{Zn_3}$ nanocluster turns it into a versatile building block which can be pre-encoded with desirable physicochemical information. This work illustrates a new approach to program dimensionality and function into stimuli-responsive atomically precise materials.

■ ASSOCIATED CONTENT

Supporting Information

The Supporting Information is available free of charge at https://pubs.acs.org/doi/10.1021/jacsau.1c00491.

Synthetic protocols, supporting characterization, and experimental data (PDF)

Accession Codes

CCDC 2102887, 2102888, 2102889, 2102890, 2102891, and 2102892 contain the supplementary crystallographic data for this paper. These data can be obtained free of charge via www.ccdc.cam.ac.uk/data_request/cif, or by emailing data_request@ccdc.cam.ac.uk, or by contacting The Cambridge Crystallographic Data Centre, 12 Union Road, Cambridge CD2 1EZ, UK; fac; + 44 1223 336033.

■ AUTHOR INFORMATION

Corresponding Author

Alexandra Velian − *Department of Chemistry, University of Washington, Seattle, Washington 98195, United States;* orcid.org/0000-0002-6782-7139; Email: avelian@uw.edu

Authors

Benjamin S. Mitchell − *Department of Chemistry, University of Washington, Seattle, Washington 98195, United States*

Sebastian M. Krajewski − *Department of Chemistry, University of Washington, Seattle, Washington 98195, United States*

Jonathan A. Kephart − *Department of Chemistry, University of Washington, Seattle, Washington 98195, United States;* orcid.org/0000-0003-4608-1160

Dylan Rogers − *Department of Chemistry, University of Washington, Seattle, Washington 98195, United States*

Werner Kaminsky − *Department of Chemistry, University of Washington, Seattle, Washington 98195, United States;* orcid.org/0000-0002-9100-4909

Complete contact information is available at: https://pubs.acs.org/10.1021/jacsau.1c00491

Notes

The authors declare no competing financial interest.

■ ACKNOWLEDGMENTS

This work was supported by the National Science Foundation (NSF) through a Faculty Early Career Development Program Award (1944843) and by the Research Corporation for Science Advancement through a Cottrell Scholars Award. The X-ray crystallography facility was funded through NSF Grant 0840520. B.S.M. is grateful for support from the NSF Graduate Research Fellowship Program. S.M.K. was supported in part through a UW Clean Energy Institute Fellowship.

■ REFERENCES

(1) Muetterties, E. L.; Rhodin, T. N.; Band, E.; Brucker, C. F.; Pretzer, W. R. Clusters and Surfaces. *Chem. Rev.* **1979**, *79* (2), 91−137.

(2) Somorjai, G. A.; Contreras, A. M.; Montano, M.; Rioux, R. M. Clusters, Surfaces, and Catalysis. *Proc. Natl. Acad. Sci. U. S. A.* **2006**, *103* (28), 10577−10583.

(3) Eames, E. V.; Betley, T. A. Site-Isolated Redox Reactivity in a Trinuclear Iron Complex. *Inorg. Chem.* **2012**, *51* (19), 10274−10278.

(4) Petel, B. E.; Brennessel, W. W.; Matson, E. M. Oxygen-Atom Vacancy Formation at Polyoxovanadate Clusters: Homogeneous Models for Reducible Metal Oxides. *J. Am. Chem. Soc.* **2018**, *140* (27), 8424−8428.

(5) Petel, B. E.; Meyer, R. L.; Maiola, M. L.; Brennessel, W. W.; Müller, A. M.; Matson, E. M. Site-Selective Halogenation of Polyoxovanadate Clusters: Atomically Precise Models for Electronic Effects of Anion Doping in VO_2. *J. Am. Chem. Soc.* **2020**, *142* (2), 1049−1056.

(6) Coucouvanis, D. Use of Preassembled Iron/Sulfur and Iron/Molybdenum/Sulfur Clusters in the Stepwise Synthesis of Potential Analogs for the Fe/Mo/S Site in Nitrogenase. *Acc. Chem. Res.* **1991**, *24* (1), 1−8.

(7) Venkateswara Rao, P.; Holm, R. H. Synthetic Analogues of the Active Sites of Iron−Sulfur Proteins. *Chem. Rev.* **2004**, *104* (2), 527−560.

(8) de Ruiter, G.; Thompson, N. B.; Lionetti, D.; Agapie, T. Nitric Oxide Activation by Distal Redox Modulation in Tetranuclear Iron Nitrosyl Complexes. *J. Am. Chem. Soc.* **2015**, *137* (44), 14094−14106.

(9) Champsaur, A. M.; Velian, A.; Paley, D. W.; Choi, B.; Roy, X.; Steigerwald, M. L.; Nuckolls, C. Building Diatomic and Triatomic Superatom Molecules. *Nano Lett.* **2016**, *16* (8), 5273−5277.

(10) Hernández Sánchez, R.; Champsaur, A.M.; Choi, B.; Wang, S.G.; Bu, W.; Roy, X.; Chen, Y.-S.; Steigerwald, M.L.; Nuckolls, C.; Paley, D.W. Electron Cartography in Clusters. *Angew. Chem., Int. Ed.* **2018**, *57* (42), 13815−13820.

(11) Nguyen, A. I.; Darago, L. E.; Balcells, D.; Tilley, T. D. Influence of a "Dangling" Co(II) Ion Bound to a $[MnCo_3O_4]$ Oxo Cubane. *J. Am. Chem. Soc.* **2018**, *140* (29), 9030−9033.

(12) McSkimming, A.; Suess, D. L. M. Selective Synthesis of Site-Differentiated Fe_4S_4 and Fe_6S_6 Clusters. *Inorg. Chem.* **2018**, *57* (23), 14904−14912.

(13) Reed, C. J.; Agapie, T. A Terminal Fe^{III}−Oxo in a Tetranuclear Cluster: Effects of Distal Metal Centers on Structure and Reactivity. *J. Am. Chem. Soc.* **2019**, *141* (24), 9479−9484.

(14) Ye, M.; Thompson, N. B.; Brown, A. C.; Suess, D. L. M. A Synthetic Model of Enzymatic $[Fe_4S_4]$−Alkyl Intermediates. *J. Am. Chem. Soc.* **2019**, *141* (34), 13330−13335.

(15) Sridharan, A.; Brown, A. C.; Suess, D. L. M. A Terminal Imido Complex of an Iron−Sulfur Cluster. *Angew. Chem., Int. Ed.* **2021**, *60* (23), 12802−12806.

(16) Grabow, L. C.; Hvolbæk, B.; Nørskov, J. K. Understanding Trends in Catalytic Activity: The Effect of Adsorbate−Adsorbate Interactions for CO Oxidation Over Transition Metals. *Top. Catal.* **2010**, *53* (5), 298−310.

(17) Qi, L.; Li, J. Adsorbate Interactions on Surface Lead to a Flattened Sabatier Volcano Plot in Reduction of Oxygen. *J. Catal.* **2012**, *295*, 59−69.
(18) Shong, B.; Bent, S. F. One-Dimensional Pattern Formation of Adsorbed Molecules on the Ge(100)-2 × 1 Surface Driven by Nearest-Neighbor Effects. *J. Phys. Chem. C* **2013**, *117* (2), 949−955.
(19) Borguet, E.; Dai, H.-L. Probing Surface Short Range Order and Inter-Adsorbate Interactions through IR Vibrational Spectroscopy:-CO on Cu (100). *J. Phys. Chem. B* **2005**, *109* (17), 8509−8512.
(20) Krishnamoorthy, A.; Yildiz, B. Quantifying the Origin of Inter-Adsorbate Interactions on Reactive Surfaces for Catalyst Screening and Design. *Phys. Chem. Chem. Phys.* **2015**, *17* (34), 22227−22234.
(21) Kephart, J. A.; Mitchell, B. S.; Chirila, A.; Anderton, K. J.; Rogers, D.; Kaminsky, W.; Velian, A. Atomically Defined Nanopropeller $Fe_3Co_6Se_8(Ph_2PNTol)_6$: Functional Model for the Electronic Metal−Support Interaction Effect and High Catalytic Activity for Carbodiimide Formation. *J. Am. Chem. Soc.* **2019**, *141* (50), 19605−19610.
(22) Kephart, J. A.; Boggiano, A. C.; Kaminsky, W.; Velian, A. Inorganic Clusters as Metalloligands: Ligand Effects on the Synthesis and Properties of Ternary Nanopropeller Clusters. *Dalton Trans* **2020**, *49* (45), 16464−16473.
(23) Kephart, J. A.; Romero, C. G.; Tseng, C.-C.; Anderton, K. J.; Yankowitz, M.; Kaminsky, W.; Velian, A. Hierarchical Nanosheets Built from Superatomic Clusters: Properties, Exfoliation and Single-Crystal-to-Single-Crystal Intercalation. *Chem. Sci.* **2020**, *11* (39), 10744−10751.
(24) Mitchell, B. S.; Kaminsky, W.; Velian, A. Tuning the Electronic Structure of Atomically Precise Sn/Co/Se Nanoclusters via Redox Matching of Tin(IV) Surface Sites. *Inorg. Chem.* **2021**, *60* (9), 6135−6139.
(25) Monod, J.; Wyman, J.; Changeux, J.-P. On the Nature of Allosteric Transitions: A Plausible Model. *J. Mol. Biol.* **1965**, *12* (1), 88−118.
(26) Changeux, J.-P. 50th Anniversary of the Word "Allosteric. *Protein Sci.* **2011**, *20* (7), 1119−1124.
(27) Cheng, H. F.; d'Aquino, A. I.; Barroso-Flores, J.; Mirkin, C. A. A Redox-Switchable, Allosteric Coordination Complex. *J. Am. Chem. Soc.* **2018**, *140* (44), 14590−14594.
(28) Lifschitz, A. M.; Rosen, M. S.; McGuirk, C. M.; Mirkin, C. A. Allosteric Supramolecular Coordination Constructs. *J. Am. Chem. Soc.* **2015**, *137* (23), 7252−7261.
(29) Lorkovic, I. M.; Wrighton, M. S.; Davis, W. M. Use of a Redox-Active Ligand to Reversibly Alter Metal Carbonyl Electrophilicity. *J. Am. Chem. Soc.* **1994**, *116* (14), 6220−6228.
(30) Cambridge Structural Database. Zn-Se distances. Accessed: 2020-05-27. 140 hits. Mean: 2.469 Å. Std Dev: 0.074 Å. Cambridge Structural Database. Zn−Se Distances. Accessed: 2020-05-27. 140 Hits. Mean: 2.469 Å. Std Dev: 0.074 Å.
(31) Bruno, I. J.; Cole, J. C.; Edgington, P. R.; Kessler, M.; Macrae, C. F.; McCabe, P.; Pearson, J.; Taylor, R. New Software for Searching the Cambridge Structural Database and Visualizing Crystal Structures. *Acta Crystallogr., Sect. B: Struct. Sci.* **2002**, *58* (3), 389−397.
(32) Groom, C. R.; Bruno, I. J.; Lightfoot, M. P.; Ward, S. C. The Cambridge Structural Database. *Acta Crystallogr., Sect. B: Struct. Sci., Cryst. Eng. Mater.* **2016**, *72* (2), 171−179.
(33) Champsaur, A. M.; Mézière, C.; Allain, M.; Paley, D. W.; Steigerwald, M. L.; Nuckolls, C.; Batail, P. Weaving Nanoscale Cloth through Electrostatic Templating. *J. Am. Chem. Soc.* **2017**, *139* (34), 11718−11721.
(34) Xie, J.; Bu, X.; Zheng, N.; Feng, P. One-Dimensional Coordination Polymers Containing Penta-Supertetrahedral Sulfide Clusters Linked by Dipyridyl Ligands. *Chem. Commun.* **2005**, *39*, 4916−4918.
(35) Vaqueiro, P.; Romero, M. L.; Rowan, B. C.; Richards, B. S. Arrays of Chiral Nanotubes and a Layered Coordination Polymer Containing Gallium−Sulfide Supertetrahedral Clusters. *Chem. - Eur. J.* **2010**, *16* (15), 4462−4465.
(36) Horwitz, N. E.; Xie, J.; Filatov, A. S.; Papoular, R. J.; Shepard, W. E.; Zee, D. Z.; Grahn, M. P.; Gilder, C.; Anderson, J. S. Redox-Active 1D Coordination Polymers of Iron−Sulfur Clusters. *J. Am. Chem. Soc.* **2019**, *141* (9), 3940−3951.
(37) Wheaton, C. A.; Puddephatt, R. J. A Coordination Polymer of Gold(I) with Heterotactic Architecture and a Comparison of the Structures of Isotactic, Syndiotactic, and Heterotactic Isomers. *Angew. Chem., Int. Ed.* **2007**, *46* (24), 4461−4463.
(38) Rasburn, J.; Foucher, D. A.; Reynolds, W. F.; Vancso, G. J. Solid State Polymerization of the Unsymmetrical [1]Ferrocenophane $Fe(\eta\text{-}C_5H_4)_2SiMePh$; Synthesis of the First Stereoregular Organometallic Polymer. *Chem. Commun.* **1998**, *7*, 843−844.
(39) Ellis, W. W.; Schmitz, M.; Arif, A. A.; Stang, P. J. Preparation, Characterization, and X-Ray Crystal Structures of Helical and Syndiotactic Zinc-Based Coordination Polymers. *Inorg. Chem.* **2000**, *39* (12), 2547−2557.
(40) Bodini, M. E.; Copia, G.; Robinson, R.; Sawyer, D. T. Redox Chemistry of Metal-Catechol Complexes in Aprotic Media. 5. 3,5-Di-Tert-Butylcatecholato and 3,5-Di-Tert-Butyl-o-Benzosemiquinonato Complexes of Zinc(II). *Inorg. Chem.* **1983**, *22* (1), 126−129.
(41) Shukla, A. D.; Das, A. Redox Responsive Binuclear Complexes Using 5,6-Dihydroxy-1,10-Phenanthroline as a Bridging Ligand: Synthesis, Characterization and Physicochemical Studies. *Polyhedron* **2000**, *19* (26), 2605−2611.
(42) Keyes, T. E.; Forster, R. J.; Jayaweera, P. M.; Coates, C. G.; McGarvey, J. J.; Vos, J. G. Modulation of Electronic Coupling across Dioxolene-Bridged Osmium and Ruthenium Dinuclear Complexes. *Inorg. Chem.* **1998**, *37* (22), 5925−5932.
(43) Schmidt, R. D.; Kent, C. A.; Concepcion, J. J.; Lin, W.; Meyer, T. J.; Forbes, M. D. E. A Little Spin on the Side: Solvent and Temperature Dependent Paramagnetism in $[Ru^{II}(Bpy)_2(Phendione)]^{2+}$. *Dalton Trans* **2014**, *43* (47), 17729−17739.

https://doi.org/10.1021/jacsau.1c00491
JACS Au 2022, 2, 92−96